PAPER

Soliton slow light for closed loop quantum systems

To cite this article: H R Hamedi *et al* 2019 *Phys. Scr.* **94** 025103

IOP Publishing | Physica Scripta
Phys. Scr. **94** (2019) 025103 (10pp) https://doi.org/10.1088/1402-4896/aafb93

Soliton slow light for closed loop quantum systems

H R Hamedi[1], M Jafari[2] and V Kudriasov[1]

[1] Institute of Theoretical Physics and Astronomy, Vilnius University, Saulėtekio 3 LT-10257 Vilnius, Lithuania
[2] Departments of Physics, K. N. Toosi University of Technology, Tehran, Iran

E-mail: hamid.hamedi@tfai.vu.lt

Received 1 October 2018, revised 17 December 2018
Accepted for publication 2 January 2019
Published 15 January 2019

Abstract

This paper describes the dynamics of solitonic pulse propagation in a closed loop quantum system comprised of five atomic energy levels. In this system four higher energy levels with four control laser fields form a closed ring-shape loop which is coherently coupled to a ground level state by a tunable probe laser field. Although the propagation of an intense probe pulse suffers losses and broadening in linear regime, there exist specific conditions where the probe pulse is found to become robust during its propagation. We attribute this regime to the formation of an optical soliton with a slow group velocity because of the balance between the dispersion and Kerr optical nonlinearity. Results obtained are based on the theoretical model using the coupled Maxwell–Bloch equations for the nonlinear propagation.

Keywords: electromagnetically induced transparency, slow light optical soliton, Kerr nonlinearity

(Some figures may appear in colour only in the online journal)

1. Introduction

The propagation of optical pulses through nonlinear media coupled coherently to one or several laser fields has been an active subject of research in various branches of physics [1–7], ranging from optical communications [8] to quantum nonlinear optics [3, 9]. The pioneering studies of the nonlinear interactions in the atomic media have opened up many new aspects in wave propagation such as slow light [10–12], coherent control of absorption and dispersion [13, 14], and large enhancement of optical nonlinearities [15–19]. In addition, a range of other remarkable optical phenomena have been investigated, such as optical bistability [20–23], quantum entanglement [24–29], storage and retrieval of light pulses [30–35], four-wave mixing [36–38], giant Kerr nonlinearity [39–43], stable optical solitons [44, 45] and so on [46–50].

Due to the nonlinearity of the medium the propagation of a light pulse may lead to a significant change in its temporal and spatial profile. However, under specific circumstances, when the balance between linear and nonlinear effects takes place, the shape of the optical pulse can be preserved over the long propagation distances. A special category of stable shape-preserving waves propagating through the nonlinear media (called solitons) can be formed as a result of balance between Kerr nonlinearity and dispersion [51]. Over the recent years, the subject of solitons has been investigated in various types of matter including cold-atoms [48, 52, 53], Bose–Einstein condensates [54, 55], and other nonlinear media [56].

Following the report of ultraslow optical solitons in a highly resonant atomic medium by Wu and Deng [44], these type of wave packets have recently attracted much attention [32, 45, 57–67]. For instance, ultraslow optical solitons, their storage and retrieval were reported in ultracold three-level Rydberg atoms [32]. The dynamics of ultraslow optical soliton in a cold, highly resonant three-state atomic system under Raman excitation has been investigated by Huang and collaborators [61]. Hang *et al* showed that a large enhancement of Kerr nonlinearity can be realized due to the appearance of a gain induced by the quantum interference in a four-level atomic system; hence a stable long distance propagation of optical solitons can be obtained with superluminal propagating velocity [66]. Due to the high potential of shape-preserving optical packets in the applications like optical information processing, more experimental studies are expected to be carried out in the near future.

So far, most of the previous studies have addressed the soliton formation using the basic atomic configurations comprising few atomic energy levels. The three basic configurations are $\Lambda-$, $\mathrm{V}-$, and the ladder-type atom-light coupling schemes [12, 17]. However, in order to achieve greater control and flexibility over the distortionless pulse propagation, novel practical schemes are required exhibiting much richer quantum interference and coherence mechanisms. Indeed, each extra atomic level impels new physical features for a particular multilevel atomic system. For instance, four-level N-type [6] and tripod [68, 69] systems have already manifested a fascinating usage in the demonstration of slow light as well as shape-preserving optical pulses [44]. More complicated level structures suggest even more charming effects because of the quantum interference and coherence induced by the extra atomic levels and the coupling light fields [11, 14, 59, 63]. In this regard, five level systems look quite promising due to both the increase in flexibility yet maintaining the reasonable complexity for the theoretical description.

To this end, a five-level toy-model atom-light coupling scheme is proposed here in which four control laser components couple a pair of internal states to another pair of states in all possible ways to establish a closed-loop setup of the atom-light interaction. A probe laser field then couples the ring-coupling structure to a ground level state. Such a scheme was first proposed by Kobrak and Rice [70] for establishing a complete population transfer [71] to a single target of a degenerate pair of states. Subsequently it has been employed to show the advantages of the measurement in coherent control of atomic or molecular processes [72]. Moreover, by using intense laser fields a new quantum measurement has been introduced in the Kobrak–Rice five-level system [73]. The Kerr nonlinearity [43] and atom localization [74] behaviors of such a configuration have been also investigated.

In our paper, we show that the nonlinear origin of the coupled Maxwell–Bloch equations describing the interaction of radiation field with such an atomic medium leads to significant effects on the behavior of pulse propagation. When the probe pulse is weak, it propagates without any significant loss and pulse shape distortion through the medium. In contrast, intense probe pulse intensity results in remarkable absorption of the probe pulse intensity through the medium accompanied by a pulse broadening after a very short propagation distance. Analytical solutions are given to elucidate such a behavior. Following this theoretical description, we investigate a different regime where a shape-preserving probe pulse propagation (soliton pulse) can be achieved. The corresponding nonlinear wave equation of the pulse propagation and the possible practical implementation of such a regime are discussed.

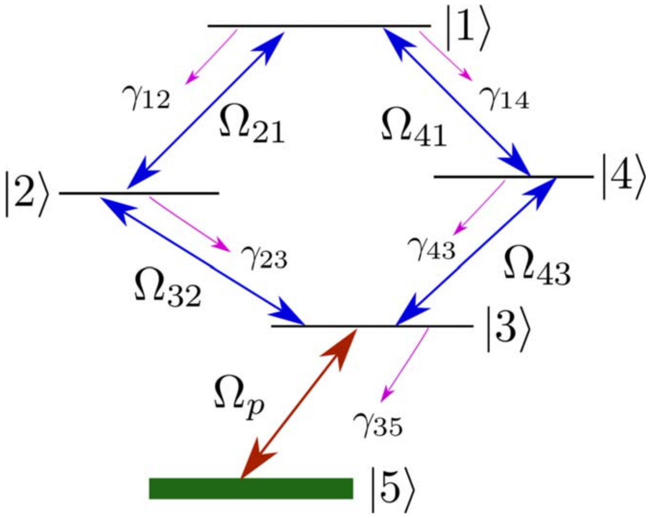

Figure 1. Schematic diagram of the five-level quantum system.

2. Model and dynamics of light propagation

Let us consider the propagation of a probe pulse by the electric field of the form

$$\overrightarrow{E_p}(z,\,t) = e_p E_p(z,\,t)\,\mathrm{e}^{\mathrm{i}(k_p z - \omega_p t)} + \mathrm{c.c}\,.. \tag{1}$$

The total electric field of control laser fields is defined as

$$\overrightarrow{E_c}(z,\,t) = e_1 E_1(z,\,t)\,\mathrm{e}^{\mathrm{i}(k_1 z - \omega_1 t)} + e_2 E_2(z,\,t)\,\mathrm{e}^{\mathrm{i}(k_2 z - \omega_2 t)} + e_3 E_3(z,\,t)\,\mathrm{e}^{\mathrm{i}(k_3 z - \omega_3 t)} + e_4 E_4(z,\,t)\,\mathrm{e}^{\mathrm{i}(k_4 z - \omega_4 t)} + \mathrm{c.c.}, \tag{2}$$

which acts as control on the propagation of probe pulse. Here, e_i and $E_i (i = p,\, 1,\, 2,\, 3,\, 4)$ are the unit polarization vector as well as the envelope of the probe and control fields, respectively. The wave number of the probe and control field is denoted by $k_i = \omega_i / c$.

We consider a level structure as illustrated in figure 1. The system consists of the excited state $|1\rangle$, two non-degenerate metastable lower states $|3\rangle, |5\rangle$ as well as two intermediate degenerate states $|4\rangle$ and $|2\rangle$. Four strong laser driving components couple a pair of atomic internal states $|1\rangle$ and $|3\rangle$ to another pair of states $|2\rangle$ and $|4\rangle$ in all possible paths making a ring-coupling structure. Such a level scheme is equivalent to a consequently coupled cyclic chain of four states $|1\rangle$, $|2\rangle$, $|3\rangle$, and $|4\rangle$ resulting in a closed-loop diamond-shape subsystem. Four Rabi-frequencies $\Omega_{21} = (e_1.\, d_{12})E_1/\hbar$, $\Omega_{23} = (e_2.\, d_{32})E_2/\hbar$, $\Omega_{41} = (e_3.\, d_{14})E_3/\hbar$, and $\Omega_{43} = (e_4.\, d_{34})E_4/\hbar (d_{ij}$ is the electric dipole matrix element corresponding to the transition $|i\rangle \leftrightarrow |j\rangle)$ are introduced to the transitions $|2\rangle \leftrightarrow |1\rangle$, $|2\rangle \leftrightarrow |3\rangle$, $|1\rangle \leftrightarrow |4\rangle$, and $|3\rangle \leftrightarrow |4\rangle$, respectively. An additional tunable coherent probe field with Rabi-frequency $\Omega_p = (e_p.\, d_{35})E_p/\hbar$ couples the diamond-shape subsystem to a ground (or metastable) state $|5\rangle$ through the dipole-allowed optical transition $|3\rangle \leftrightarrow |5\rangle$.

The total Hamiltonian of the system H_{TS} can be written as

$$H_{\mathrm{TS}} = -\hbar(\Omega_p|3\rangle\langle 5| + \Omega_{41}|1\rangle e^{i\phi}\langle 4| + \Omega_{21}|2\rangle\langle 1| + \Omega_{32}|3\rangle\langle 2| + \Omega_{43}|4\rangle\langle 3|) + \text{h.c.}, \quad (3)$$

where $\phi = \phi_{41} + \phi_{43} + \phi_{32} + \phi_{21}$ denotes the relative phase accumulated after completing a ring, while ϕ_{ij} describes the initial phase of each laser field.

The atomic motion is modeled by the density operator

$$\dot{\rho} = -\frac{i}{\hbar}[H_{\mathrm{TS}}, \rho] + L_\rho, \quad (4)$$

where L_ρ stands for the damping operator represented the decay of the system. Substituting equation (3) into equation (4), the optical Bloch equations for density matrix elements describing the evolution of the system are obtained and are presented in appendix A.

Maxwell equation controls the evolution of the electric field $\vec{E} = \vec{E}_p + \vec{E}_c$ in the system

$$\nabla^2\vec{E} - \frac{1}{c^2}\frac{\partial^2}{\partial t^2}\vec{E} = \frac{1}{\varepsilon_0 c^2}\frac{\partial^2}{\partial t^2}\vec{P}, \quad (5)$$

with the optical polarization

$$\vec{P} = N(d_{53}\rho_{35}e^{i(k_p z-\omega_p t)} + d_{12}\rho_{21}e^{i(k_1 z-\omega_1 t)} + d_{32}\rho_{23}\, e^{i(k_2 z-\omega_2 t)} + d_{14}\rho_{41}e^{i(k_3 z-\omega_3 t)} + d_{43}\rho_{34}e^{i(k_4 z-\omega_4 t)} + \text{c.c}), \quad (6)$$

with N being the atomic density.

Working in the slowly varying envelope approximation, one can obtain the temporal and spatial evolution of the probe pulse as

$$\frac{\partial\Omega_p}{\partial z} + \frac{\partial\Omega_p}{c\partial t} = iq\rho_{35}, \quad (7)$$

where $q = 2N\omega_p|d_{35}|^2/\hbar c$ is the propagation coupling constant. The solution of Maxwell–Bloch equations (4) and (7) describes the propagation dynamics of probe pulse inside the medium.

3. Linear pulse propagation

In the following, we discuss the linear evolution of probe field propagating through the five-level atomic system. The solution of the nonlinearity coupled equations (4) and (7) enables us to model also the nonlinear propagation of the probe pulse and provide a rather precise picture of interplay between the dispersion and nonlinearities inside such a five-level system which will be studied in next section. However, before solving these equations for the nonlinear regime we first examine the linear behavior of the system by presenting some numerical results. This may give some effective hints for the study of nonlinear pulse propagation discussed later. In doing so, we assume that the atom is initially in ground state $|5\rangle$, and that the Rabi-frequency of the probe pulse is small enough (compared to the Raby-frequencies of control fields) so that we can neglect the depletion of the ground level. Therefore, we can apply the perturbation expansion $\rho_{ij} = \rho_{ij}^{(0)} + \rho_{ij}^{(1)} + \rho_{ij}^{(2)} + ...$ where ρ_{ij}^{m} is the mth-order of ρ_{ij} in terms of probe pulse Ω_p. The zeroth order solution is $\rho_{55}^{(0)} = 1$ while other elements being zero. Keeping up to the first order of Ω_p, the set of consequential equations from Maxwell–Bloch equations (4) and (7) can be reduced under linearization to the form

$$\dot{\rho}_{15}^{(1)} = -g_1\rho_{15}^{(1)} + i\Omega_{41}e^{i\phi}\rho_{45}^{(1)} + i\Omega_{21}\rho_{25}^{(1)}, \quad (8a)$$

$$\dot{\rho}_{25}^{(1)} = -g_2\rho_{25}^{(1)} + i\Omega_{21}\rho_{15}^{(1)} + i\Omega_{32}\rho_{35}^{(1)}, \quad (8b)$$

$$\dot{\rho}_{35}^{(1)} = -g_3\rho_{35}^{(1)}, +i\Omega_{43}\rho_{45}^{(1)} + i\Omega_{32}\rho_{25}^{(1)} + i\Omega_p, \quad (8c)$$

$$\dot{\rho}_{45}^{(1)} = -g_4\rho_{45}^{(1)} + i\Omega_{41}e^{-i\phi}\rho_{15}^{(1)} + i\Omega_{43}\rho_{35}^{(1)}, \quad (8d)$$

and

$$\frac{\partial\Omega_p}{\partial z} + \frac{\partial\Omega_p}{c\partial t} = iq\rho_{35}^{(1)}. \quad (9)$$

Performing the time Fourier transform of equations (8) and (9), we get

$$G_1(\omega)Y_{15}^{(1)} + \Omega_{41}e^{i\phi}Y_{45}^{(1)} + \Omega_{21}Y_{25}^{(1)} = 0, \quad (10a)$$

$$G_2(\omega)Y_{25}^{(1)} + \Omega_{21}Y_{15}^{(1)} + \Omega_{32}Y_{35}^{(1)} = 0, \quad (10b)$$

$$G_3(\omega)Y_{35}^{(1)} + \Omega_{43}Y_{45}^{(1)} + \Omega_{32}Y_{25}^{(1)} + \varpi_p = 0, \quad (10c)$$

$$G_4(\omega)Y_{45}^{(1)} + \Omega_{41}e^{-i\phi}Y_{15}^{(1)} + \Omega_{43}Y_{35}^{(1)} = 0, \quad (10d)$$

and

$$\frac{\partial\varpi_p}{\partial z} - i\frac{\omega}{c}\varpi_p = iqY_{35}^{(1)}, \quad (11)$$

where $G_1(\omega) = [\omega + (\Delta_{14} + \Delta_{43} + \Delta_p) + i(\gamma_{14} + \gamma_{12})]$, $G_2(\omega) = [\omega + (\Delta_{23} - \Delta + \Delta_p) + i\gamma_{23}]$, $G_3(\omega) = (\omega + i\gamma_{35} + \Delta_p)$, and $G_4(\omega) = [\omega - (\Delta_{43} + \Delta_p) - i\gamma_{43}]$. Note that ϖ_p and $Y_{ij}^{(1)}$ represent the Fourier transform of Ω_p and $\rho_{ij}^{(1)}$, respectively, while ω is the Fourier transform variable.

Equations (10*a*)–(10*d*) can be solved analytically, yielding

$$Y_{35}^{(1)} = \frac{\varpi_p}{L(\omega)}L_1(\omega), \quad (12a)$$

$$Y_{45}^{(1)} = -\frac{\varpi_p}{L(\omega)}L_2(\omega), \quad (12b)$$

$$Y_{25}^{(1)} = -\frac{\varpi_p}{L(\omega)}L_3(\omega), \quad (12c)$$

$$Y_{15}^{(1)} = \frac{\varpi_p}{L(\omega)}L_4(\omega), \quad (12d)$$

where

$$L_1(\omega) = G_1(\omega)G_2(\omega)G_4(\omega) - G_4(\omega)\Omega_{21}^2 - G_2(\omega)\Omega_{41}^2, \quad (13a)$$

$$L_2(\omega) = \Omega_{32}\Omega_{21}\Omega_{41}e^{-i\phi} - \Omega_{43}\Omega_{21}^2 + \Omega_{43}G_1(\omega)G_2(\omega), \quad (13b)$$

$$L_3(\omega) = \Omega_{43}\Omega_{41}\Omega_{21}e^{i\phi} - \Omega_{32}\Omega_{41}^2 + \Omega_{32}G_1(\omega)G_4(\omega), \quad (13c)$$

$$L_4(\omega) = \Omega_{32}\Omega_{21}G_4(\omega) + \Omega_{43}\Omega_{41}e^{i\phi}G_2(\omega), \quad (13d)$$

and

$$
\begin{aligned}
L(\omega) = {} & \Omega_{43}^2 G_1(\omega) G_2(\omega) - \Omega_{32}^2 \Omega_{41}^2 - \Omega_{43}^2 \Omega_{21}^2 \\
& + \Omega_{32}^2 G_1(\omega) G_4(\omega) + \Omega_{21}^2 G_3(\omega) G_4(\omega) \\
& + \Omega_{41}^2 G_2(\omega) G_3(\omega) - G_1(\omega) G_2(\omega) G_3(\omega) G_4(\omega) \\
& + 2\Omega_{43}\Omega_{32}\Omega_{21}\Omega_{41} \cos\phi. \qquad (14)
\end{aligned}
$$

A solution of equation (11) is plane wave of the form

$$\varpi_p(z, \omega) = \varpi_p(0, \omega) \mathrm{e}^{\mathrm{i}\kappa(\omega) z}, \qquad (15)$$

where

$$\kappa(\omega) = \frac{\omega}{c} - q\frac{L_1(\omega)}{L(\omega)}, \qquad (16)$$

describes the linear dispersion relation of the system. Expanding $\kappa(\omega)$ in power series around the center frequency of the probe pulse and taking the first three terms, we get

$$\kappa(\omega) = \kappa_0 + \kappa_1 \omega + \kappa_2 \omega^2, \qquad (17)$$

with

$$\kappa_0 = -q\frac{L_1}{L}, \qquad (18a)$$

$$\kappa_1 = \frac{1}{c} - q\left(\frac{Q}{L} - \frac{L_1 B}{L^2}\right), \qquad (18b)$$

$$\kappa_2 = q\left[L_1\left(-\frac{1}{SL^2} + \frac{2}{BL^3}\right) + \frac{R}{L} - \frac{2Q}{BL^2}\right], \qquad (18c)$$

where the detailed expressions for Q, B, S and R are given in appendix B, while L and L_1 can be obtained by substituting $\omega = 0$ into equations (13*a*) and (14) for $L(\omega)$ and $L_1(\omega)$, respectively. In equation (17), $\kappa_i = \frac{\partial^2 \kappa(\omega)}{\partial \omega^2}|_{\omega=0} (i = 0, 1, 2)$ gives the dispersion coefficients in different orders. In general, for $\kappa_0 = \Phi + \mathrm{i}\alpha/2$ the real part corresponds to the phase shift Φ per unit length, while the imaginary part describes the absorption α of the probe pulse. The group velocity is $v_g = 1/\kappa_1$, and the nonlinear term κ_2 is associated with group velocity dispersion and leads to pulse distortion during the propagation.

4. Influence of Kerr nonlinearity

The linear response of the atomic medium is now obtained through neglecting higher-order terms of the probe field and under the weak-field approximation. However, it is known that for the intense probe pulses the nonlinear factors due to the inherent Kerr nonlinearity of the system must be also taken into account. It is due to the significant impact of the nonlinearity of the system in high powers of probe pulse which may lead to probe attenuation and distortion. To have a better understanding of this, the propagation problem is simulated by solving simultaneously the coupled Maxwell–Bloch equations for the five-level closed loop system. We work in the retarded frame with the traveling coordinates $t' = t - z/c$, $z' = z$. This choice of coordinates reduces the partial differential equation (7) with respect to the independent variable z'

$$\frac{\partial \Omega_p}{\partial z'} = \mathrm{i}q\rho_{35}. \qquad (19)$$

We assume the propagation of a Gaussian probe pulse

$$\Omega_p(0, t') = \Omega_p^0 \mathrm{e}^{-(t'/\tau_0)^2}, \qquad (20)$$

where τ_0 is the temporal width of the input pulse (its time duration).

In order to investigate the impact of nonlinearities on pulse propagation stemming from strong power of probe pulse, we assume the four control fields as continuous waves and all the Rabi-frequencies are the same

$$\Omega_{43} = \Omega_{23} = \Omega_{41} = \Omega_{21} = \Omega. \qquad (21)$$

In what follows, we present our numerical results. Without loss of generality, we take $\gamma_{43} = \gamma_{23} = \gamma_{12} = \gamma_{14} = \gamma_{35} = \gamma$ [74]. Figure 2 shows the resulting propagation dynamics of a weak Gaussian probe pulse through the five-level quantum system for different values of relative phase ϕ while $\Omega_p^0 = 0.01\gamma$. It can be seen from figures 2(a)–(c) that the relative phase ϕ can seriously affect the absorption of the pulse. The case with $\phi = 0$ (figure 2(a)) gives rise to the loss of the weak probe pulse intensity through the medium after almost a short propagation distance. In contrast and as can be observed from figures 2(b) and (c), when $\phi = \pi/2$ and $\phi = \pi$ the weak probe pulse is transmitted through the phase-sensitive system almost without any substantial absorption and broadening while it can still keep its shape for quite a long propagation distance.

Such a phase-sensitive behavior can be elucidated through the following analytical model.

Without the ground state $|5\rangle$ in equation (3), the Hamiltonian of the atom-light interaction for the remaining atomic four-level closed-loop level structure of the ring-coupling subsystem H_{SS} simplifies to ($\hbar = 1$):

$$H_{\mathrm{SS}} = -\Omega\left[|1\rangle \mathrm{e}^{\mathrm{i}\phi}\langle 4| + \sum_{j=1}^{3} |j+1\rangle\langle j| + \mathrm{h.c}\right]. \qquad (22)$$

In writing equation (22) the Rabi-frequencies are chosen according to equation (21).

Following [43, 74], the eigenenergies for the Hamiltonian equation (22) can be expressed as

$$E_n = -2\Omega \cos\lambda_n, \qquad (23)$$

with $\lambda_n = \frac{n\pi}{2} - \frac{\pi}{2} - \frac{\phi}{4}$, where $(n = 1, 2, 3, 4)$.

Let us now inspect the eigenenergies in the limiting cases depending on the relative phase ϕ.

(i) The case where $\phi = 0$. In this situation, equation (23) reduces to

$$E_n = -2\Omega \sin\left(\frac{n\pi}{2}\right). \qquad (24)$$

Equation (24) results in three eigenenergies $E_3 = -E_1 = 2\Omega$, and $E_2 = E_4 = 0$. In this case the

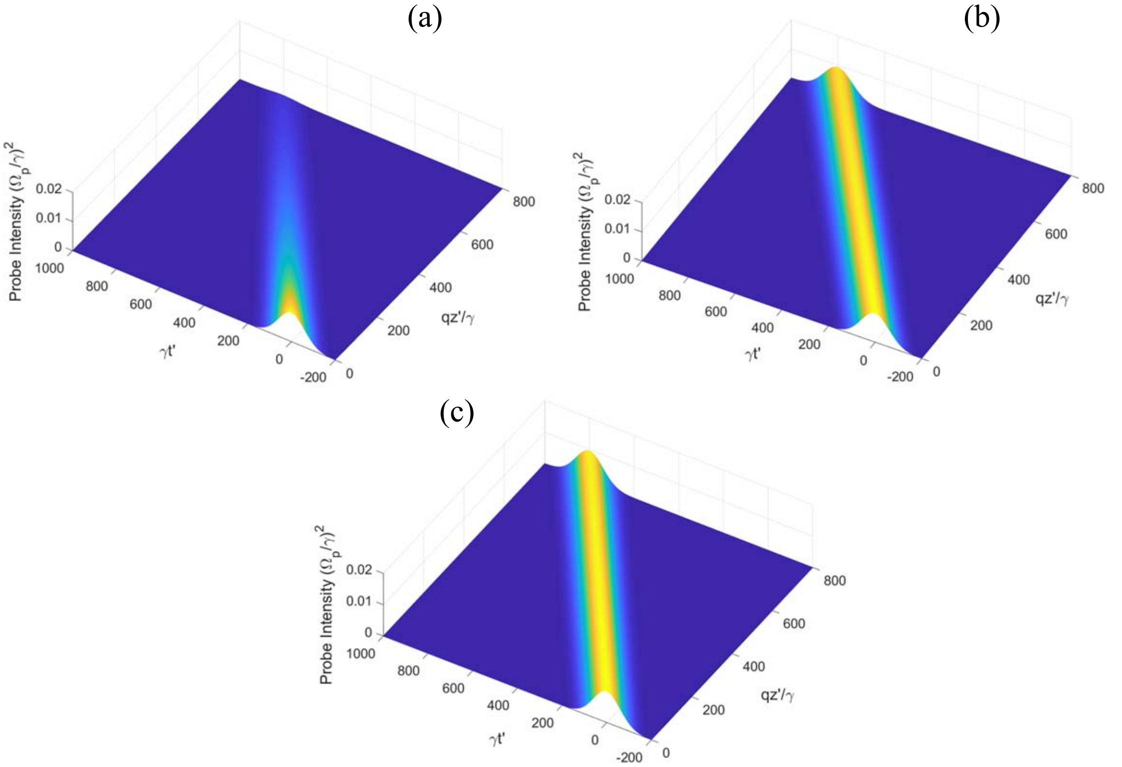

Figure 2. Propagation dynamics of a Gaussian probe pulse with $\Omega_p^0 = 0.01\gamma$ and (a) $\phi = 0$, (b) $\phi = \pi/2$, (c) $\phi = \pi$. The other parameters are $\gamma_{14} = \gamma_{12} = \gamma_{23} = \gamma_{43} = \gamma_{35} = \gamma$, $\Delta = \Delta_{12} = \Delta_{14} = \Delta_{23} = \Delta_{43} = \Delta_p = 0$, $\Omega_{43} = \Omega_{23} = \Omega_{41} = \Omega_{21} = \Omega = 10\gamma$ and $\tau_0 = 60/\gamma$.

lowest energy eigenstate corresponding to $E_1 = -2\Omega$ is not degenerate.

(ii) The case where $\phi = \pi/2$. If $\phi = \pi/2$, then

$$E_n = -2\Omega \sin\left(\frac{n\pi}{2} - \frac{\pi}{8}\right), \tag{25}$$

resulting in $E_3 = -E_1 = 4\Omega \cos\frac{\pi}{8}$, and $E_4 = -E_2 = 4\Omega \sin\frac{\pi}{8}$.

(iii) The case where $\phi = \pi$. In this case, equation (23) changes to

$$E_n = -2\Omega \sin\left(\frac{n\pi}{2} - \frac{\pi}{4}\right), \tag{26}$$

giving rise to two pairs of degenerate eigenenergies $E_1 = E_2 = -\sqrt{2}\,\Omega$ and $E_3 = E_4 = \sqrt{2}\,\Omega$ separated by the energy $2\sqrt{2}\,\Omega$.

Figure 3 illustrates the density plot of probe absorption against the probe detuning Δ_p and the relative phase ϕ. One can see that three, four and two absorption peaks appear for $\phi = 0$, $\phi = \pi/2$, and $\phi = \pi$, respectively. Obviously, the medium experiences an absorption peak at zero probe detuning for $\phi = 0$ which may result in pulse attenuation during its propagation, as was observed in figure 2(a). However, for cases $\phi = \pi/2$ and $\phi = \pi$, the medium is transparent at $\Delta_p = 0$, leading to a distortionless transmission of light pulse (see also figures 2(b) and (c)) [43]. This indicates an optical switching between absorption and transparency through relative phase of applied fields [43].

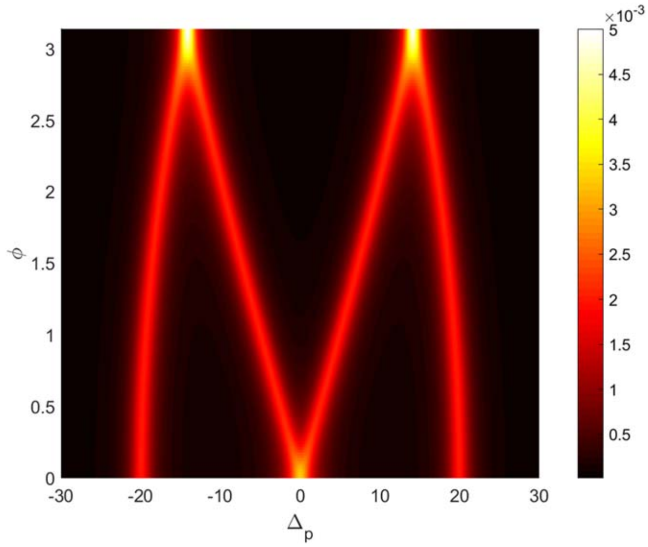

Figure 3. Density plot of probe absorption against Δ_p and ϕ for the same parameters as figure 2.

Now, we investigate the propagation of probe pulses with higher intensities. This is the situation where the effect of nonlinearities becomes important. The propagation dynamics of an intense probe pulse with $\Omega_p^0 = \gamma$ is plotted in figure 4 for different values of ϕ for the same parameters as used in figure 2. Clearly, the intense probe pulse is strongly attenuated by the medium even more rapidly with respect to figure 2(a) (figure 4(a)). The interesting results are obtained for the cases $\phi = \pi/2$ (figure 4(b)) and $\phi = \pi$ (figure 4(c)).

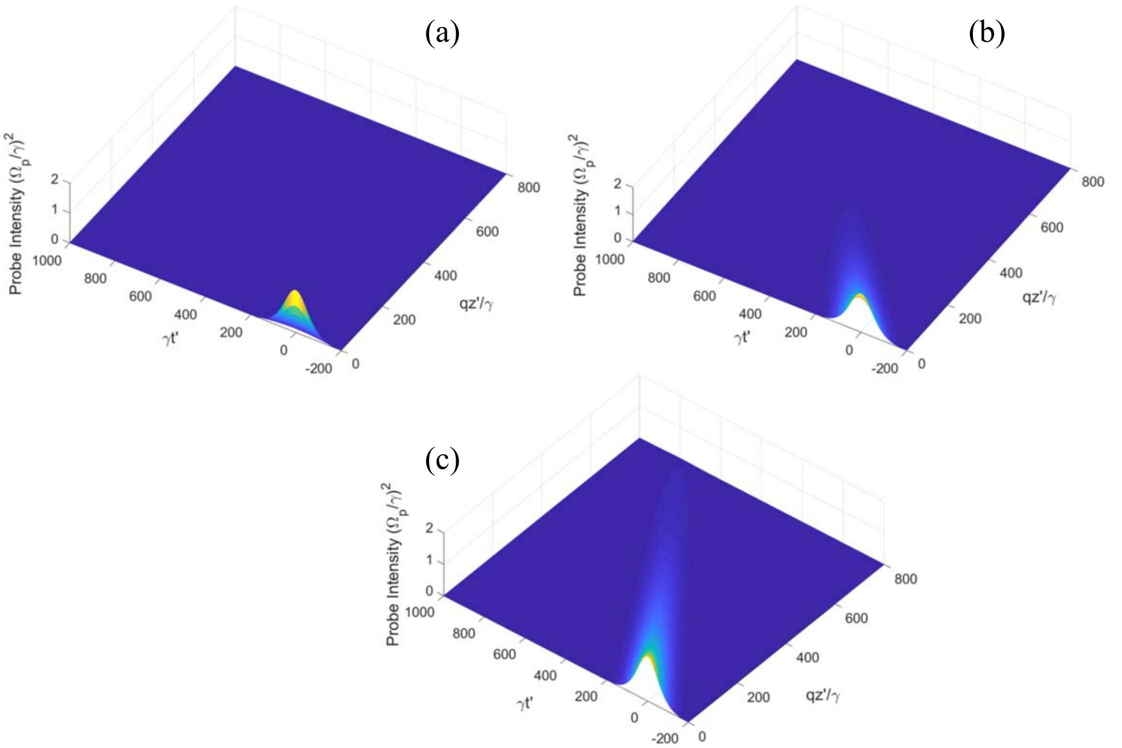

Figure 4. Propagation dynamics of a Gaussian probe pulse with $\Omega_p^0 = \gamma$ and (a) $\phi = 0$, (b) $\phi = \pi/2$, (c) $\phi = \pi$. The other parameters are the same as figure 2.

Evidently, in both situations the intense probe pulse suffers strong absorption and broadening during the propagating through the closed-loop medium.

In a linear regime and for a Gaussian shape incoming probe pulse of the form $\Omega_p(0, t) = \Omega_p^0 \mathrm{e}^{-(t/\tau_0)^2}$ with a duration τ_0, the time evolution of probe pulse after carrying out an inverse Fourier transform is $\Omega_p(z, t) = \frac{\Omega_p^0}{\sqrt{x}} \exp\left[\mathrm{i}\kappa_0 z - \frac{(t - \kappa_1 z)^2}{x\tau_0^2}\right]$ where $x = u_1 - \mathrm{i}u_2$, $u_1 = 1 + 4z\,\mathrm{Re}(\kappa_2)/\tau_0^2$ and $u_2 = 4z\mathrm{Im}(\kappa_2)/\tau_0^2$. Therefore, even in absence of the absorption effects in the medium ($\mathrm{Im}(\kappa_i) = 0$) the dispersion effects take part to the spreading and attenuation of the pulse during propagation. This is a key result indicating that at higher intensities the dispersion effects may contribute in pulse distortion and attenuation. We aim at obtaining the shape-preserving and lossless optical pulses propagating inside the medium. In order to compensate the dispersion effects, in next section we include the Kerr nonlinearity of probe pulse into the pulse propagation which results in robust and shape preserving optical pulses.

5. Soliton regime

In what follows we turn to study the nonlinear evolution of the probe pulse through the phase sensitive atomic structure. In order to investigate the nonlinear propagation of light, one needs to evaluate the nonlinear effects induced by Kerr nonlinearity, which is due to nonlinear terms up to the third order of Ω_p. According to [44], we take a trial function

$$\varpi_p(z, \omega) = \tilde{\varpi}_p(z, \omega)\mathrm{e}^{\mathrm{i}\kappa_0 z}. \tag{27}$$

Substituting equation (27) into wave equation (11) and using equation (17) we obtain

$$\frac{\partial \varpi_p}{\partial z} = \mathrm{i}(\kappa_1\omega + \kappa_2\omega^2)\varpi_p, \tag{28}$$

where we only kept terms up to the order ω^2 in expanding the dispersion relation $\kappa(\omega)$. Note that here we have replaced ϖ_p with $\tilde{\varpi}_p$ for the sake of convenience. Since we are interested in nonlinear evolution of light, we must take into account the nonlinear polarization of the probe pulse by the form $\mathrm{i}\eta\rho_{35} \to \mathrm{i}\eta\rho_{35}^{(1)} + \mathrm{i}\chi_{\mathrm{NL}}$ where the nonlinear term is

$$\chi_{\mathrm{NL}} = -q\mathrm{e}^{-\mathrm{i}\kappa_0 z}\rho_{35}^{(1)}\sum_{i=1}^{4}\rho_{i5}^{(1)}, \tag{29}$$

and $\rho_{i5}^{(1)}$ can be obtained by taking $\omega = 0$ in equations (12*a*)–(12*d*). Reminding $\kappa_1 = v_g^{-1}$ and after carrying out inverse transform, equation (28) takes the form

$$-\mathrm{i}\left[\frac{\partial}{\partial z} + v_g^{-1}\frac{\partial}{\partial t}\right]\Omega_p + \kappa_2\frac{\partial^2}{\partial t^2}\Omega_p = \chi_{\mathrm{NL}}. \tag{30}$$

Defining new coordinates $\zeta = z$ and $\eta = t - z/v_g$, we arrive at the nonlinear wave function of slowly varying envelope Ω_p as

$$\mathrm{i}\frac{\partial}{\partial\zeta}\Omega_p - \kappa_2\frac{\partial^2}{\partial\eta^2}\Omega_p = N\mathrm{e}^{-\alpha\zeta}|\Omega_p|^2\Omega_p, \tag{31}$$

with $\alpha = 2\mathrm{Im}(\kappa_0)$ being the absorption coefficient. The nonlinear coefficient N of probe pulse proportional to nonlinear Kerr susceptibility is defined by

$$N = \frac{-q}{L|L|^2}(G_1 G_2 G_4 - G_4 \Omega_{21}^2 - G_2 \Omega_{41}^2) \times (\Psi_1 + \Psi_2 + \Psi_3 + \Psi_4), \quad (32)$$

where the coefficients Ψ_1, Ψ_2, Ψ_3 and Ψ_4 are presented in appendix C.

Equation (31) has generally complex coefficients. However, the absorption coefficient α may be very small for some specific parametric values, i.e. $\alpha \approx 0$, and the real parts of the complex coefficients may become much larger than the corresponding imaginary parts

$$\kappa_2 = \kappa_{2R} + i\kappa_{2I} \approx \kappa_{2R}, \quad (33)$$

and

$$N = N_R + iN_I \approx N_R. \quad (34)$$

In this case, we get

$$i\frac{\partial}{\partial \zeta}\Omega_p - \kappa_{2R}\frac{\partial^2}{\partial \eta^2}\Omega_p = N_R|\Omega_p|^2\Omega_p. \quad (35)$$

Equation (35) is the well-known nonlinear Schrodinger equation (NSE) which governs the nonlinear pulse propagation, which is well studied in fiber optics [75]. Similar equation was deduced, for example, in [44, 45] in cold three- and four- state atomic structures. Although the five-level atomic structure consider in this work and the three- and four-level schemes in [44, 45] reduce to the same NSE, however, our proposed scheme has some advantages over the previously studied configurations. A main advantage of our proposed model is the phase sensitivity of our proposed scheme, as discussed in details in section 4. In addition, as a result of the quantum interference and coherence induced by the extra atomic levels and the coupling light fields, such a five-level scheme can result in larger magnitude of the Kerr nonlinearity with respect to the three and four-level counterparts [43].

Depending on the sign of $\kappa_{2R}N_R$, equation (35) allows bright and dark soliton solutions. A bright soliton is obtained when $\kappa_{2R}N_R$ is positive

$$\Omega_p = \Omega_{p0}\text{sech}[\eta/\tau]\exp(-i\zeta N_R|\Omega_p|^2\Omega_p), \quad (36)$$

while a dark soliton is expected when $\kappa_{2R}N_R$ is negative

$$\Omega_p = \Omega_{p0}\tanh[\eta/\tau]\exp(-i\zeta N_R|\Omega_p|^2\Omega_p). \quad (37)$$

It should be pointed out that $\Omega_{p0} = (1/\tau)(\kappa_{2R}/N_R)^{1/2}$ denotes the typical Rabi-frequency of the probe field and τ is the typical pulse duration.

Next we give a numerical example for the formation of the shape preserving optical solitons. The proposed level structure can be experimentally implemented using the ^{87}Rb atoms. The ground level $|5\rangle$ can be assigned to the state $5S_{1/2}$. The level $|3\rangle$ can be attributed to the $5P_{3/2}$. Two intermediate levels $|2\rangle$ and $|4\rangle$ can be assigned to either the fine structure of the $4D_{3/2}$ or the $4D_{5/2}$ sub-states, as long as the dipole transition selection rules on the F quantum number is satisfied (the same F quantum number for the intermediate states). The top level $|1\rangle$ can be chosen to the $6P_{3/2}$ state. Taking

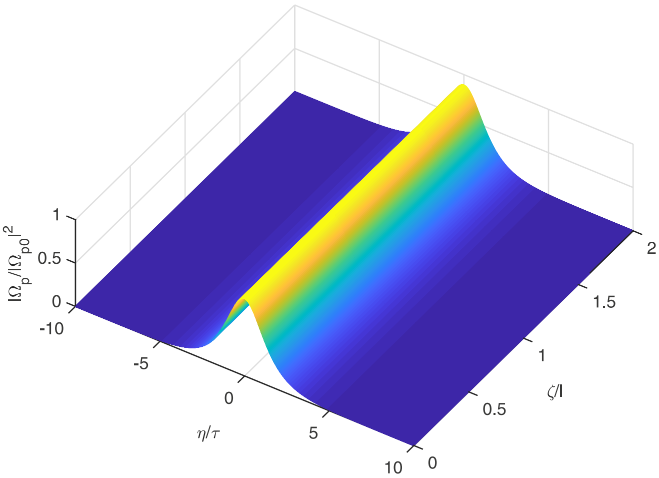

Figure 5. Propagation dynamics of a slow optical soliton with $\tau = 10^{-9}$ s, $l = 1$ cm and the parameters given in the main text.

$\gamma_{21} = \gamma_{23} = \gamma_{43} = \gamma_{53} = \gamma = 3.7 \times 10^7\ \text{s}^{-1}$ [74], $\tau = 10^{-9}$ s, $q = 10^{10}\ \text{cm}^{-1}\ \text{s}^{-1}$, $\Omega_{21} = \Omega_{41} = \Omega_{43} = \Omega_{32} = \Omega = 2.59 \times 10^9\ \text{s}^{-1}$, $\Delta_{12} = 2.96 \times 10^9\ \text{s}^{-1}$, $\Delta_{14} = 1.11 \times 10^9\ \text{s}^{-1}$, $\Delta_{43} = 1.85 \times 10^9$, $\Delta_{23} = 1.48 \times 10^9$, $\Delta_p = 0$, and $\phi = \pi$, one can obtain $\kappa_1 = (9.44 + 7.7 \times 10^{-2}i) \times 10^{-10}\ \text{cm}^{-1}$ s, $\kappa_2 = (1.02 - 6.5 \times 10^{-3}i) \times 10^{-19}\ \text{cm}^{-1}$ s, $N = (2.39 - 6.95 \times 10^{-2}i) \times 10^{-20}\ \text{cm}^{-1}\ \text{s}^2$. Clearly, the imaginary parts of the complex coefficients are much smaller than the corresponding real parts. Thus, the conditions (33) and (34) are satisfied. In this situation, the standard NSE (35) with $\kappa_{2R}N_R > 0$ is well characterized, leading to the generation of bright solitons in the proposed system. Such a soliton has a width and amplitude satisfying $|\Omega_{p0}\tau| \approx 2.06$. With the above system parameters, one can find $v_g \approx 3.5 \times 10^{-2}c$, indicating that the soliton propagates with a slow propagating velocity. As can be observed from figure 5, such a bright soliton remains fairly stable during propagation, which may be due to the balance between the group velocity dispersion and Kerr-type nonlinearity.

6. Concluding remarks

In conclusion, the problem of pulse propagation has been theoretically investigated for a five-level toy-model atom-light coupling system in which the probe laser beam couples a ground level to the ring-coupling subsystem consisting of four atomic energy levels. We have found that the distortionless propagation of the probe pulse without significant absorption and broadening is possible in the linear regime when the intensity of the probe pulse is sufficiently weak. In contrast, for higher intensities, the probe pulse will be attenuated by the medium after almost a short propagation distance. We then presented an analytical model to elucidate the origin of such behavior. By employing a simple theoretical model for the nonlinear pulse propagation, we found the regime of stable distortionless probe pulses propagation through such a medium. Based on the coupled Maxwell–Bloch equations, a nonlinear equation governing the evolution of the probe pulse envelope has been obtained showing the existence of stable optical solitons with a slow propagating velocity. The formation of these shape-preserving optical solitons has been attributed to the balance between dispersion and Kerr nonlinearity of the system. A possible experimental realization of the investigated model has been proposed for the ^{87}Rb atomic medium with suitable parameters.

As a result of the quantum interference and coherence effects induced by the extra atomic levels and the coupling light fields in such a five level atomic structure, the proposed atomic model has potential applications for establishing a complete population transfer to a single target of a degenerate pair of states [71], or high precision and high resolution localization of an atom [74]. The obtained results may be helpful for guiding experimental investigations of linear and nonlinear optical properties of atomic systems and for applications of optical information processing and engineering.

Acknowledgments

HRH gratefully acknowledges the support by the European Social Fund under grant No. 09.3.3-LMT-K-712-01-0051. The authors gratefully acknowledge S H Asadpour for helpful discussions on nonlinear light propagation.

Appendix A. Explicit expressions of the optical Bloch equation

Under the rotating wave approximation, the equation of motion (4) for the density operator describing the atomic system reduces to

$$\dot{\rho}_{15} = -g_1\rho_{15} + \mathrm{i}\Omega_{41}\mathrm{e}^{\mathrm{i}\phi}\rho_{45} - \mathrm{i}\Omega_p\rho_{13} + \mathrm{i}\Omega_{21}\rho_{25}, \quad \text{(A1)}$$

$$\dot{\rho}_{25} = -g_2\rho_{25} + \mathrm{i}\Omega_{21}\rho_{15} + \mathrm{i}\Omega_{32}\rho_{35} - \mathrm{i}\Omega_p\rho_{23}, \quad \text{(A2)}$$

$$\dot{\rho}_{35} = -g_3\rho_{35} + \mathrm{i}\Omega_{43}\rho_{45} + \mathrm{i}\Omega_{32}\rho_{25} + \mathrm{i}\Omega_p(\rho_{55} - \rho_{33}), \quad \text{(A3)}$$

$$\dot{\rho}_{45} = -g_4\rho_{45} + \mathrm{i}\Omega_{41}\mathrm{e}^{-\mathrm{i}\phi}\rho_{15} + \mathrm{i}\Omega_{43}\rho_{35} - \mathrm{i}\Omega_p\rho_{43}, \quad \text{(A4)}$$

$$\dot{\rho}_{41} = -g_5\rho_{41} + \mathrm{i}\Omega_{41}\mathrm{e}^{-\mathrm{i}\phi}(\rho_{11} - \rho_{44}) + \mathrm{i}\Omega_{43}\rho_{31} - \mathrm{i}\Omega_{21}\rho_{42}, \quad \text{(A5)}$$

$$\dot{\rho}_{42} = -g_6\rho_{42} + \mathrm{i}\Omega_{41}\mathrm{e}^{-\mathrm{i}\phi}\rho_{12} + \mathrm{i}\Omega_{43}\rho_{32} - \mathrm{i}\Omega_{32}\rho_{43} - \mathrm{i}\Omega_{21}\rho_{41}, \quad \text{(A6)}$$

$$\dot{\rho}_{43} = -g_7\rho_{43} + \mathrm{i}\Omega_{41}\mathrm{e}^{-\mathrm{i}\phi}\rho_{13} + \mathrm{i}\Omega_{43}(\rho_{33} - \rho_{44}) - \mathrm{i}\Omega_{32}\rho_{42} - \mathrm{i}\Omega_p\rho_{45}, \quad \text{(A7)}$$

$$\dot{\rho}_{21} = -g_8\rho_{21} - \mathrm{i}\Omega_{41}\mathrm{e}^{-\mathrm{i}\phi}\rho_{24} + \mathrm{i}\Omega_{21}(\rho_{11} - \rho_{22}) + \mathrm{i}\Omega_{32}\rho_{31}, \quad \text{(A8)}$$

$$\dot{\rho}_{23} = -g_9\rho_{23} + \mathrm{i}\Omega_{21}\rho_{13} + \mathrm{i}\Omega_{32}(\rho_{33} - \rho_{22}) - \mathrm{i}\Omega_{43}\rho_{24} - \mathrm{i}\Omega_p\rho_{25}, \quad \text{(A9)}$$

$$\dot{\rho}_{31} = -g_{10}\rho_{31} + \mathrm{i}\Omega_{32}\rho_{21} + \mathrm{i}\Omega_p\rho_{51} - \mathrm{i}\Omega_{41}\mathrm{e}^{-\mathrm{i}\phi}\rho_{34} + \mathrm{i}\Omega_{43}\rho_{41} - \mathrm{i}\Omega_{21}\rho_{32}, \quad \text{(A10)}$$

$$\dot{\rho}_{11} = -2(\gamma_{14} + \gamma_{12})\rho_{11} + \mathrm{i}\Omega_{41}(\mathrm{e}^{\mathrm{i}\phi}\rho_{41} - \mathrm{e}^{-\mathrm{i}\phi}\rho_{14}) - \mathrm{i}\Omega_{21}(\rho_{12} - \rho_{21}), \quad \text{(A11)}$$

$$\dot{\rho}_{22} = 2\gamma_{12}\rho_{11} - 2\gamma_{23}\rho_{22} + \mathrm{i}\Omega_{32}(\rho_{32} - \rho_{23}) + \mathrm{i}\Omega_{21}(\rho_{12} - \rho_{21}), \quad \text{(A12)}$$

$$\dot{\rho}_{33} = 2\gamma_{43}\rho_{44} + 2\gamma_{23}\rho_{22} - 2\gamma_{35}\rho_{33} + \mathrm{i}\Omega_{43}(\rho_{43} - \rho_{34}) + \mathrm{i}\Omega_{32}(\rho_{23} - \rho_{32}) - \mathrm{i}\Omega_p(\rho_{35} - \rho_{53}), \quad \text{(A13)}$$

$$\dot{\rho}_{44} = 2\gamma_{14}\rho_{11} - 2\gamma_{43}\rho_{44} - \mathrm{i}\Omega_{43}(\rho_{43} - \rho_{34}) - \mathrm{i}\Omega_{41}(\mathrm{e}^{\mathrm{i}\phi}\rho_{41} - \mathrm{e}^{-\mathrm{i}\phi}\rho_{14}), \quad \text{(A14)}$$

$$\rho_{11} + \rho_{22} + \rho_{33} + \rho_{44} + \rho_{55} = 1, \quad \text{(A15)}$$

with $g_1 = [-\mathrm{i}(\Delta_{14} + \Delta_{43} + \Delta_p) + (\gamma_{14} + \gamma_{12})]$, $g_2 = [-\mathrm{i}(\Delta_{23} - \Delta + \Delta_p) + \gamma_{23}]$, $g_3 = (\gamma_{35} - \mathrm{i}\Delta_p)$, $g_4 = [\mathrm{i}(\Delta_{43} + \Delta_p) - \gamma_{43}]$, $g_5 = [\mathrm{i}\Delta_{14} + (\gamma_{43} + \gamma_{14} + \gamma_{12})]$, $g_6 = [-\mathrm{i}(\Delta_{12} - \Delta_{14}) + (\gamma_{43} + \gamma_{23})]$, $g_7 = [-\mathrm{i}\Delta_{43} + \gamma_{43} + \gamma_{35}]$, $g_8 = [\mathrm{i}\Delta_{12} + (\gamma_{14} + \gamma_{12} + \gamma_{23})]$, $g_9 = [-\mathrm{i}(\Delta_{12} - \Delta) + \gamma_{23}]$ and $g_{10} = [\mathrm{i}(\Delta_{14} + \Delta_{43}) + (\gamma_{14} + \gamma_{12})]$. The one-photon resonance detuning parameters for transitions $|4\rangle \leftrightarrow |3\rangle$, $|2\rangle \leftrightarrow |3\rangle$, $|1\rangle \leftrightarrow |4\rangle$, $|2\rangle \leftrightarrow |1\rangle$ and $|3\rangle \leftrightarrow |5\rangle$ are $\Delta_{43} = \omega_4 - \omega_{43}$, $\Delta_{23} = \omega_2 - \omega_{23}$, $\Delta_{14} = \omega_3 - \omega_{14}$, $\Delta_{12} = \omega_1 - \omega_{12}$, and $\Delta_p = \omega_p - \omega_{35}$, while $\Delta = \Delta_{12} - \Delta_{14} + \Delta_{23} - \Delta_{43}$ and ω_i represent the multi-photon detuning and the central frequency of the corresponding laser field. The spontaneous decays from the excited state $|1\rangle$ to the lower levels $|3\rangle$ and $|5\rangle$ are ignored due to the assumption that the corresponding transitions are dipole forbidden. The spontaneous decay rates of upper level $|i\rangle$ to the lower level $|j\rangle$ is described by $2\gamma_{ij}$.

Appendix B. Explicit expressions of Q, B, S and R

Expressions for Q, B, S and R read

$$Q = \Omega_{21}^2 + \Omega_{41}^2 - G_4G_1 - G_2G_1 - G_2G_4, \quad \text{(B1)}$$

$$B = \Omega_{32}^2G_4 + \Omega_{32}^2G_1 + \Omega_{43}^2G_2 + \Omega_{43}^2G_4 + \Omega_{21}^2G_1 + \Omega_{21}^2G_3 + \Omega_{41}^2G_2 + \Omega_{41}^2G_3 - G_3G_4G_1 - G_3G_2G_1 - G_3G_4G_2 - G_2G_4G_1, \quad \text{(B2)}$$

$$S = -2(\Omega_{21}^2 + \Omega_{32}^2 + \Omega_{41}^2 + \Omega_{43}^2 + G_2G_1 + G_3G_1 + G_2G_4 + G_3G_4 + G_2G_3 + G_1G_4), \quad \text{(B3)}$$

$$R = 2\Delta_{14} - 2\Delta + 2\Delta_{23} + 2\Delta_p + 2\mathrm{i}(\gamma_{23} - \gamma_{43}), \quad \text{(B4)}$$

where G_1, G_2, G_3, G_4, L and L_1 can be obtained by substituting $\omega = 0$ in coefficients $G_1(\omega)$, $G_2(\omega)$, $G_3(\omega)$, $G_4(\omega)$, $L(\omega)$ and $L_1(\omega)$, respectively.

Appendix C. Explicit expressions of Ψ_1, Ψ_2, Ψ_3 and Ψ_4

Expressions for Ψ_1, Ψ_2, Ψ_3 and Ψ_4 can be expressed as

$$\begin{aligned}\Psi_1 &= G_1 G_1^* G_2^* G_2 G_4 G_4^* - \Omega_{21}^2 G_1 G_2 G_4 G_4^* \\ &- \Omega_{41}^2 G_1 G_2 G_4 G_2^* - \Omega_{21}^2 G_4 G_1^* G_2^* G_4^* + \Omega_{21}^4 G_4 G_4^* \\ &+ \Omega_{21}^2 \Omega_{41}^2 G_4 G_2^* - \Omega_{41}^2 G_2 G_1^* G_2^* G_4^* + \Omega_{21}^2 \Omega_{41}^2 G_2 G_4^* \\ &+ \Omega_{41}^4 G_2 G_2^*,\end{aligned} \tag{C1}$$

$$\begin{aligned}\Psi_2 &= \Omega_{32}^2 \Omega_{21}^2 \Omega_{41}^2 - 2\Omega_{32}\Omega_{43}\Omega_{21}^3\Omega_{41}\cos\phi \\ &+ \Omega_{43}^2\Omega_{21}^4 + \Omega_{43}\Omega_{21}\Omega_{32}\Omega_{41}\mathrm{e}^{\mathrm{i}\phi} G_1 G_2 \\ &+ \Omega_{32}\Omega_{21}\Omega_{43}\Omega_{41}\mathrm{e}^{-\mathrm{i}\phi} G_1^* G_2^* - \Omega_{43}^2\Omega_{21}^2 G_1^* G_2^* \\ &- \Omega_{43}^2\Omega_{21}^2 G_1 G_2 + \Omega_{43}^2 G_1 G_1^* G_2^* G_2^*,\end{aligned} \tag{C2}$$

$$\begin{aligned}\Psi_3 &= \Omega_{43}^2\Omega_{21}^2\Omega_{41}^2 - 2\Omega_{43}\Omega_{21}\Omega_{32}\Omega_{41}^3\cos\phi + \Omega_{32}^2\Omega_{41}^4 \\ &+ \Omega_{43}\Omega_{32}\Omega_{21}\Omega_{41}\mathrm{e}^{-\mathrm{i}\phi} G_1 G_4 + \Omega_{43}\Omega_{21}\Omega_{32}\Omega_{41}\mathrm{e}^{\mathrm{i}\phi} G_1^* G_4^* \\ &- \Omega_{32}^2\Omega_{41}^2 G_1^* G_4^* - \Omega_{32}^2\Omega_{41}^2 G_1 G_4 + \Omega_{32}^2 G_1 G_1^* G_4 G_4^*,\end{aligned} \tag{C3}$$

$$\begin{aligned}\Psi_4 &= \Omega_{32}^2\Omega_{21}^2 G_4 G_4^* + \Omega_{32}\Omega_{21}\Omega_{43}\Omega_{41}\mathrm{e}^{-\mathrm{i}\phi} G_2^* G_4 \\ &+ \Omega_{32}\Omega_{21}\Omega_{43}\Omega_{41}\mathrm{e}^{\mathrm{i}\phi} G_4^* G_2 + \Omega_{43}^2\Omega_{41}^2 G_2 G_2^*.\end{aligned} \tag{C4}$$

ORCID iDs

H R Hamedi https://orcid.org/0000-0003-4370-4158

References

[1] Clader B D and Eberly J H 2007 Two-pulse propagation in media with quantum-mixed ground states *Phys. Rev.* A **76** 053812
[2] Fleischhauer M and Manka A S 1996 Propagation of laser pulses and coherent population transfer in dissipative three-level systems: an adiabatic dressed-state picture *Phys. Rev.* A **54** 794–803
[3] Grobe R, Hioe F T and Eberly J H 1994 Formation of shape-preserving pulses in a nonlinear adiabatically integrable system *Phys. Rev. Lett.* **73** 3183–6
[4] Csesznegi J R and Grobe R 1997 Recall and creation of spatial excitation distributions in dielectric media *Phys. Rev. Lett.* **79** 3162–5
[5] Mazets I E 2005 Adiabatic pulse propagation in coherent atomic media with the tripod level configuration *Phys. Rev.* A **71** 023806
[6] Rajitha K V, Tarak N D, Evers J and Kiffner M 2015 Pulse splitting in light propagation through N-type atomic media due to an interplay of Kerr nonlinearity and group-velocity dispersion *Phys. Rev.* A **92** 023840
[7] Xiao Y, Maywar D N and Agrawal G P 2012 New approach to pulse propagation in nonlinear dispersive optical media *J. Opt. Soc. Am.* **29** 2958
[8] Haus H A and Wong W S 1996 Solitons in optical communications *Rev. Mod. Phys.* **68** 423–44
[9] McCall S L and Hahn E L 1967 Self-induced transparency by pulsed coherent light *Phys. Rev. Lett.* **18** 908–11
[10] Fleischhauer M and Lukin M D 2000 Dark-state polaritons in electromagnetically induced transparency *Phys. Rev. Lett.* **84** 5094
[11] Paspalakis E and Knight P L 2002 Electromagnetically induced transparency and controlled group velocity in a multilevel system *Phys. Rev.* A **66** 015802
[12] Wu Y and Yang X 2005 Electromagnetically induced transparency in V-, Λ-, and cascade-type schemes beyond steady-state analysis *Phys. Rev.* A **71** 053806
[13] Li L, Guo H, Xiao F, Peng X and Chen X 2005 Control of light in an M-type five-level atomic system *J. Opt. Soc. Am.* B **22** 1309–13
[14] Sahrai M, Tajalli H, Kapale K T and Zubairy M S 2004 Tunable phase control for subluminal to superluminal light propagation *Phys. Rev.* A **70** 023813
[15] Harris S E and Hau L V 1999 Nonlinear optics at low light levels *Phys. Rev. Lett.* **82** 4611
[16] Lukin M D and Imamoğlu A 2000 Nonlinear optics and quantum entanglement of ultraslow single photons *Phys. Rev. Lett.* **84** 1419
[17] Fleischhauer M, Imamoglu A and Marangos J P 2005 Electromagnetically induced transparency: optics in coherent media *Rev. Mod. Phys.* **77** 633
[18] Kang H and Zhu Y 2003 Observation of large Kerr nonlinearity at low light intensities *Phys. Rev. Lett.* **91** 093601
[19] Petrosyan D and Malakyan Y P 2004 Magneto-optical rotation and cross-phase modulation via coherently driven four-level atoms in a tripod configuration *Phys. Rev.* A **70** 023822
[20] Joshi A, Brown A, Wang H and Xiao M 2003 Controlling optical bistability in a three-level atomic system *Phys. Rev.* A **67** 041801(R)
[21] Li J-H, Lü X-Y, Luo J-M and Huang Q-J 2006 Optical bistability and multistability via atomic coherence in an N-type atomic medium *Phys. Rev.* A **74** 035801
[22] Wang Z and Yu B 2013 Optical bistability via dual electromagnetically induced transparency in a coupled quantum-well nanostructure *J. Appl. Phys.* **113** 113101
[23] Wang Z, Chen A-X, Bai Y, Yang W-X and Lee R-K 2012 Coherent control of optical bistability in an open Λ-type three-level atomic system *J. Opt. Soc. Am.* B **29** 2891–6
[24] Wu Y, Payne M G, Hagley E W and Deng L 2004 Preparation of multiparty entangled states using pairwise perfectly efficient single-probe photon four-wave mixing *Phys. Rev.* A **69** 063803
[25] Jing H, Liu X-J, Ge M-L and Zhan M-S 2005 Correlated quantum memory: manipulating atomic entanglement via electromagnetically induced transparency *Phys. Rev.* A **71** 062336
[26] Hu X-m and Zou J-h 2008 Quantum-beat lasers as bright sources of entangled sub-Poissonian light *Phys. Rev.* A **78** 045801
[27] Li G-x, Ke S-s and Ficek Z 2009 Generation of pure continuous-variable entangled cluster states of four separate atomic ensembles in a ring cavity *Phys. Rev.* A **79** 033827
[28] Tan H-t, Xia H-x and Li G-x 2009 Interference-induced enhancement of field entanglement from an intracavity three-level V-type atom *Phys. Rev.* A **79** 063805
[29] Liu S, Li J, Yu R and Wu Y 2013 Achieving three-dimensional entanglement between two spatially separated atoms by using the quantum Zeno effect *Phys. Rev.* A **87** 062316
[30] Dey T N and Agarwal G S 2003 Storage and retrieval of light pulses at moderate powers *Phys. Rev.* A **67** 033813
[31] Ruseckas J, Yu I A and Juzeliūnas G 2017 Creation of two-photon states via interactions between Rydberg atoms during light storage *Phys. Rev.* A **95** 023807
[32] Chen Y, Bai Z and Huang G 2014 Ultraslow optical solitons and their storage and retrieval in an ultracold ladder-type atomic system *Phys. Rev.* A **89** 023835

[33] Chen Z, Bai Z, Li H-j, Hang C and Huang G 2015 Storage and retrieval of (3 + 1)-dimensional weak-light bullets and vortices in a coherent atomic gas *Sci. Rep.* **5** 8211
[34] Phillips D F, Fleischhauer A, Mair A, Walsworth R L and Lukin M D 2001 Storage of light in atomic vapor *Phys. Rev. Lett.* **86** 783
[35] Fleischhauer M and Lukin M D 2002 Quantum memory for photons: dark-state polaritons *Phys. Rev.* A **65** 022314
[36] Li Y-q and Xiao M 1996 Enhancement of nondegenerate four-wave mixing based on electromagnetically induced transparency in rubidium atoms *Opt. Lett.* **21** 1064–6
[37] Wu Y, Yang X, Sun C P, Zhou X J and Wang Y Q 2000 Theory of four-wave mixing with matter waves without the undepleted pump approximation *Phys. Rev.* A **61** 043604
[38] Wu Y, Saldana J and Zhu Y 2003 Large enhancement of four-wave mixing by suppression of photon absorption from electromagnetically induced transparency *Phys. Rev.* A **67** 013811
[39] Wang H, Goorskey D and Xiao M 2001 Enhanced Kerr nonlinearity via atomic coherence in a three-level atomic system *Phys. Rev. Lett.* **87** 073601
[40] Niu Y and Gong S 2006 Enhancing Kerr nonlinearity via spontaneously generated coherence *Phys. Rev.* A **73** 053811
[41] Yang X, Li S, Zhang C and Wang H 2009 Enhanced cross-Kerr nonlinearity via electromagnetically induced transparency in a four-level tripod atomic system *J. Opt. Soc. Am.* B **26** 1423–34
[42] Sheng J, Yang X, Wu H and Xiao M 2011 Modified self-Kerr-nonlinearity in a four-level N-type atomic system *Phys. Rev.* A **84** 053820
[43] Hamedi H R and Juzeliūnas G 2015 Phase-sensitive Kerr nonlinearity for closed-loop quantum systems *Phys. Rev.* A **91** 053823
[44] Wu Y and Deng L 2004 Ultraslow optical solitons in a cold four-state medium *Phys. Rev. Lett.* **93** 143904
[45] Wu Y and Deng L 2004 Ultraslow bright and dark optical solitons in a cold three-state medium *Opt. Lett.* **29** 2064–6
[46] Wang M, Hang C and Huang G 2018 Nonlinear propagation of four components with different polarizations and frequencies in a single optical pulse by using a five-level atomic system *J. Opt. Soc. Am.* B **35** 2217–27
[47] Tuan A N, Le Van D and Huy B N 2018 Manipulating multi-frequency light in a five-level cascade-type atomic medium associated with giant self-Kerr nonlinearity *J. Opt. Soc. Am.* B **35** 1233–9
[48] Das A, Das B C, Chakrabarti S, Bhattacharyya D and De S 2018 Observation and theoretical simulation of dispersive properties of an electromagnetically induced transparent 87Rb atomic medium *Laser Phys.* **28** 125205
[49] Yang S-J, Rui J, Dai H-N, Jin X-M, Chen S and Pan J-W 2018 High-contrast transparency comb of the electromagnetically-induced-transparency memory *Phys. Rev.* A **98** 033802
[50] Liu Q and Tan C 2018 Coherent control of subluminal optical solitons by the incoherent pumping in a ladder-type atomic system *Eur. Phys. J.* D **72** 99
[51] Hasegawa A and Tappert F 1973 Transmission of stationary nonlinear optical pulses in dispersive dielectric fibers. I. anomalous dispersion *Appl. Phys. Lett.* **23** 142
[52] Liu X-J, Jing H and Ge M-L 2004 Solitons formed by dark-state polaritons in an electromagnetic induced transparency *Phys. Rev.* A **70** 055802
[53] Xie X-T, Li W-B and Yang W-X 2006 Slow bistable solitons in a cold three-state medium *J. Phys. B: At. Mol. Opt. Phys.* **39** 401
[54] Burger S, Bongs K, Dettmer S, Ertmer W, Sengstock K, Sanpera A, Shlyapnikov G V and Lewenstein M 1999 Dark solitons in bose–einstein condensates *Phys. Rev. Lett.* **83** 5198
[55] Huang G, Szeftel J and Zhu S 2002 Dynamics of dark solitons in quasi-one-dimensional Bose–Einstein condensates *Phys. Rev.* A **65** 053605
[56] Xie X-T, Li W, Li J, Yang W-X, Yuan A and Yang X 2007 Transverse acoustic wave in molecular magnets via electromagnetically induced transparency *Phys. Rev.* B **75** 184423
[57] Yang W-X, Hou J-M, Lin Y Y and Lee R-K 2009 Detuning management of optical solitons in coupled quantum wells *Phys. Rev.* A **79** 033825
[58] Hang C, Huang G and Deng L 2006 Stable high-dimensional spatial weak-light solitons in a resonant three-state atomic system *Phys. Rev.* E **74** 046601
[59] Si L-G, Yang W-X, Liu J-B, Li J and Yang X 2009 Slow vector optical solitons in a cold five-level hyper V-type atomic system *Opt. Express* **17** 7771–83
[60] Yang W-X, Chen A-X, Lee R-K and Wu Y 2011 Matched slow optical soliton pairs via biexciton coherence in quantum dots *Phys. Rev.* A **84** 013835
[61] Huang G, Deng L and Payne M G 2005 Dynamics of ultraslow optical solitons in a cold three-state atomic system *Phys. Rev.* E **72** 016617
[62] Zhu C and Huang G 2011 High-order nonlinear Schrödinger equation and weak-light superluminal solitons in active Raman gain media with two control fields *Opt. Express* **19** 1963–74
[63] Si L-G, Yang W-X, Lü X-Y, Hao X and Yang X 2010 Formation and propagation of ultraslow three-wave-vector optical solitons in a cold seven-level triple-Λ atomic system under Raman excitation *Phys. Rev.* A **82** 013836
[64] Liu J-B, Liu N, Shan C-J, Liu T-K and Huang Y-X 2010 Slow optical soliton pairs via electron spin coherence in a quantum well waveguide *Phys. Rev.* E **81** 036607
[65] Li L and Huang G 2010 Linear and nonlinear light propagations in a Doppler-broadened medium via electromagnetically induced transparency *Phys. Rev.* A **82** 023809
[66] Hang C and Huang G 2010 Giant Kerr nonlinearity and weak-light superluminal optical solitons in a four-state atomic system with gain doublet *Opt. Express* **18** 2952–66
[67] Li B, Qi Y, Niu Y and Gong S 2015 Superluminal optical vector solitons in a five-level M-type atomic system *J. Phys. B: At. Mol. Opt. Phys.* **48** 065501
[68] Chen Y, Chen Z and Huang G 2015 Storage and retrieval of vector optical solitons via double electromagnetically induced transparency *Phys. Rev.* A **91** 023820
[69] Ruseckas J, Mekys A and Juzeliūnas G 2011 Slow polaritons with orbital angular momentum in atomic gases *Phys. Rev.* A **83** 023812
[70] Kobrak M N and Rice S A 1998 Selective photochemistry via adiabatic passage: an extension of stimulated Raman adiabatic passage for degenerate final states *Phys. Rev.* A **57** 2885
[71] Bergmann K, Theuer H and Shore B W 1998 Coherent population transfer among quantum states of atoms and molecules *Rev. Mod. Phys.* **70** 1003
[72] Jiangbin Gong and Rice S A 2004 Measurement-assisted coherent control *J. Chem. Phys.* **120** 9984
[73] Sugawara M 2006 Measurement-assisted quantum dynamics control of 5-level system using intense CW-laser fields *Chem. Phys. Lett.* **428** 457–60
[74] Hamedi H R and Juzeliūnas G 2016 Phase-sensitive atom localization for closed-loop quantum systems *Phys. Rev.* A **94** 013842
[75] Agrawal G P 2001 *Nonlinear Fiber Optics* 3th edn (New York: Academic) ch 5